Environ. Sci. Technol. **2011,** *45,* 762–768

Differential Gene Expression in *Daphnia magna* Suggests Distinct Modes of Action and Bioavailability for ZnO Nanoparticles and Zn Ions

HELEN C. POYNTON,*,† JAMES M. LAZORCHAK,† CHRISTOPHER A. IMPELLITTERI,‡ MARK E. SMITH,§ KIM ROGERS,‖ MANOMITA PATRA,‖ KATHERINE A. HAMMER,§ H. JOEL ALLEN,‡ AND CHRIS D. VULPE⊥

National Exposure Research Laboratory, U.S. Environmental Protection Agency, Cincinnati, Ohio, United States, National Risk Management Research Laboratory, U.S. Environmental Protection Agency, Cincinnati, Ohio, United States, The McConnell Group, Inc., Cincinnati, Ohio, United States, National Exposure Research Laboratory, U.S. Environmental Protection Agency, Las Vegas, Nevada, United States, and Department of Nutritional Sciences and Toxicology, University of California, Berkeley, California, United States

Received July 22, 2010. Revised manuscript received November 1, 2010. Accepted November 18, 2010.

Zinc oxide nanoparticles (ZnO NPs) are being rapidly developed for use in consumer products, wastewater treatment, and chemotherapy providing several possible routes for ZnO NP exposure to humans and aquatic organisms. Recent studies have shown that ZnO NPs undergo rapid dissolution to Zn^{2+}, but the relative contribution of Zn^{2+} to ZnO NP bioavailability and toxicity is not clear. We show that a fraction of the ZnO NPs in suspension dissolves, and this fraction cannot account for the toxicity of the ZnO NP suspensions to *Daphnia magna.* Gene expression profiling of *D. magna* exposed to ZnO NPs or $ZnSO_4$ at sublethal concentrations revealed distinct modes of toxicity. There was also little overlap in gene expression between ZnO NPs and SiO_x NPs, suggesting specificity for the ZnO NP expression profile. ZnO NPs effected expression of genes involved in cytoskeletal transport, cellular respiration, and reproduction. A specific pattern of differential expression of three biomarker genes including a multicystatin, ferritin, and C1q containing gene were confirmed for ZnO NP exposure and provide a suite of biomarkers for identifying environmental exposure to ZnO NPs and differentiating between NP and ionic exposure.

* Corresponding author. Present address: Environmental, Earth and Ocean Sciences, University of Massachusetts, 100 Morrissey Blvd., Boston, MA 02125, United States. Phone: (617) 287-7323; fax: (617) 287-7474; e-mail: helen.poynton@umb.edu.

† National Exposure Research Laboratory, U.S. Environmental Protection Agency, Cincinnati.

‡ National Risk Management Research Laboratory, U.S. Environmental Protection Agency.

§ The McConnell Group, Inc.

‖ National Exposure Research Laboratory, U.S. Environmental Protection Agency, Las Vegas.

⊥ University of California, Berkeley.

Introduction

The past decade has seen exponential growth in nanotechnology, raising concerns that production of new nanomaterials is surpassing our ability to assess their potential environmental risks (www.nanotechproject.org). Nanoparticles (NPs) are defined as supramolecular compounds or composites in the "nano" range (having at least two dimensions less than 100 nm). Although they are composed of materials well studied in toxicology, their small size often alters their chemical and physical properties and may result in unexpected toxicity (*1, 2*). Additionally, NPs constitute a very diverse range of materials creating unique challenges to risk assessors who must consider the risks posed by each material and understand how chemical alterations affect this risk (*3*).

As with most industrial products, NPs are expected to enter the aquatic environment, and many of these particles are bioavailable and can exhibit toxicity (*1*). Hassellov et al. recently reviewed several of the analytical techniques available for detecting and characterizing nanomaterials in aqueous media (*4*). However, to date, most studies have been performed in simple water systems that do not reflect the complexity of environmental samples. Samples containing naturally occurring organic matter and colloids may interfere with the detection of nanoparticles making it difficult to accurately quantify concentrations of engineered nanoparticles (*2*). Because of these complexities, accurately measuring nanoparticle exposure to organisms is difficult.

ZnO NPs are utilized in numerous commercial products including paints, cosmetics, and sunscreens primarily due to their protection against UV radiation (*5*). They have also been proposed for use in water disinfection and chemotherapy because of their selective toxicity toward bacteria and cancerous cells (*6, 7*). Given these applications, there is a high exposure potential for humans and aquatic organisms to ZnO NPs. Recent studies have suggested that the toxicity of ZnO nanoparticles is due to Zn ions released from particles through dissolution. Franklin et al. demonstrated by dialysis and filtration that ZnO NPs are soluble, resulting in toxicity to microalgae (*8*). Others studies with *Daphnia magna* have attributed ZnO NP toxicity to dissolution of Zn^{2+} through the use of a bacterial biosensor (*9*). However, studies in plants (*10*), the copepod *Tigriopus japonicus* (*11*), and zebrafish embryos (*12*) imply that dissolution does not account for the total observed toxicity of ZnO NPs to these organisms and that Zn ions and ZnO NPs have distinct modes of action (MOA). Understanding the relative contribution of Zn^{2+} to the bioavailability and toxicity of ZnO NPs is essential for preventing exposure and protecting ecosystems.

Genomic tools such as DNA microarrays may aid in detecting environmental exposure to NPs and help determine if toxicity is due to the NPs or ions present following dissolution (*13*). Griffitt et al. used gene expression to successfully discriminate between different metal NPs and their metal ions (*14*). In addition, gene expression analysis has been used to identify biomarkers of exposure and detect casual agents in field samples (*15*). The aim of this study is to use gene expression analysis to determine if the toxicity of ZnO NPs to the aquatic crustacean *D. magna* is due to dissolution of NPs and identify biomarkers of nanoparticle exposure that may be developed to specifically detect NP exposure in the environment, distinguishing between NP and ion exposure and between different NPs.

Materials and Methods

Preparation of Metal Salt Solutions and Nanoparticle Suspensions. Zinc sulfate heptahydrate (101% purity, Sigma-

10.1021/es102501z

Published on Web 12/13/2010

TABLE 1. Acute Toxicity of ZnO Nanoparticles to *Daphnia magna*[a]

chemical exposure	toxicity values			exposure concentrations	
	LC_{10} (mg/L)	LC_{25} (mg/L)	LC_{50} (mg/L)	low ($^1/_{10}$ LC_{50}) (mg/L)	high (LC_{25}) (mg/L)
Zn^{2+} as $ZnSO_4$	0.68 ± 0.41	0.91 ± 0.45	1.28 ± 0.40	0.13	0.91
ZnO particles	3.7 ± 1.8	9.0 ± 5.5	22.0 ± 12.2	2.2	9.0
SiO_x particles	NP	NP	NP	1.4[b]	5.1[c]

[a] Daphnids were exposed to $ZnSO_4$ or ZnO nanoparticles for 24 h. Following exposure the number of surviving individuals, defined as remaining mobile after mild agitation, were counted, and toxicity values were calculated using inhibition concentration percentage estimates (Icp). Toxicity values were averaged over three independent tests and are shown above with standard deviation. These toxicity values were used to determine exposure concentrations at $^1/_{10}$ LC_{50} and LC_{25}. Toxicity tests were not performed with the SiO_x nanoparticles and are represented in the table as "NP". [b] The concentration of SiO_x particles used for the $^1/_{10}$ LC_{50} exposure corresponds to the equivalent molar concentration of the ZnO particles at the $^1/_{10}$ LC_{50}. [c] The concentration of SiO_x particles used for the LC_{25} exposure corresponds to the equivalent molar concentration of ZnO particles at LC_{25}.

Aldrich, St. Louis, MO) stock solutions were prepared by direct addition into deionized water. The following nanopowders were obtained from NanoAmor Inc. (Houston, TX): 20 nm zinc oxide (ZnO) (uncoated) nanopowder and 15 nm nonporous silicon dioxide (SiO_x; $x \sim 1.2$) (uncoated) nanopowder. Stock suspensions were prepared in moderately hard reconstituted water (MHRW) (*16*) by adding the nanopowder to the MHRW during constant stirring. Stock suspensions were prepared in the experimental media (MHRW) because nanoparticle properties (e.g., aggregation and possible dissolution) may differ in deionized water and MHRW. Suspensions were sonicated using a Fisher Scientific FS20 sonicator for 10 min, stirred, and then allowed to settle for 5 min. The top 75% (approximately) of the suspension was drawn off and placed in a clean beaker and again stirred. The bottom portion of the suspension consisting of large, visible particle aggregates was discarded to reduce the presence of aggregates outside of the nano range, which would be difficult to resuspend in the exposure conditions. Three 50 mL aliquots of each suspension were taken and analyzed for Zn content.

Transmission Electron Microscopy. Nanoparticle suspensions were characterized using transmission electron microscopy (TEM) to investigate particle size and confirm elemental composition of the nanoparticles. Nanoparticles were visualized at 10 nm resolution on a Tecnai G^2 F30 S-TWIN transmission electron microscope. Energy dispersive X-ray spectroscopy (EDS) was used to determine the elemental composition of the sample. Average particle diameter and size distribution were determined by analyzing TEM images using Image-Pro Plus 7.0 (Media Cybernetics, Bethesda, MD). The diameters of approximately 100 ZnO particles and 50 SiO_x particles were measured in three images to estimate the average particle size.

Analytical Methods To Determine Metal Content. Fifty milliliter samples were collected from nanoparticle stock suspensions after preparation and before and after each bioassay and exposure. Samples were acidified with trace metal grade nitric acid (Fisher Scientific, Pittsburgh, PA) and digested based on EPA Method 3051 (*17*). Inductively coupled plasma optical emission spectroscopy (ICP-OES, Optima 2100, Perkin-Elmer, Shelton, CT) was used to determine Zn concentrations.

***D. magna* Acute Toxicity Bioassays.** Acute toxicity assays were conducted using protocols similar to the U.S. EPA Whole Effluent Toxicity (WET) protocol (*16*). Details on culture maintenance and water quality parameters monitored during the test are available in the Supporting Information. *D. magna* were placed in 50 mL of MHRW containing varying concentrations of nanoparticle suspension or metal ion for 24 h. Each treatment was slowly bubbled at an approximate rate of 2 bubbles/second during the exposure to maintain suspensions. At this rate, bubbling did not adversely affect daphnids or reduce survival in control treatments. Five concentrations and a zero concentration control, each with four replicates, were tested for each contaminant. The LC_{10}, LC_{25}, and LC_{50} were determined using the linear interpolation method as described by the U.S. EPA (*18*). Each bioassay was repeated at least three times on separate dates.

Nanoparticle Exposures. Sixteen adult (10 day old) *D. magna* were exposed to a sublethal (1/10th LC_{50}) or an approaching lethal (LC_{25}) concentration of $ZnSO_4$ or ZnO NPs for 24 h (see Table 1 for exposure concentrations) with slow bubbling as described above. The LC_{25} is the highest exposure concentration possible to ensure adequate live organisms for downstream gene expression analysis. *D. magna* were also exposed to SiO_x NPs at an equimolar concentration to the ZnO NPs to serve as a NP control. SiO_x NPs were selected for use in this study because they have low toxicity compared with ZnO NPs (*19*). An untreated exposure was performed alongside each chemical treatment to provide a matched control for microarray analysis. The treatments were repeated three times on separate dates to provide three biologic replicates for each concentration for microarray analysis. Four additional independent exposures were performed for biomarker confirmation using reverse transcription PCR.

Ultrafiltration. Ultrafiltration was performed to determine extent of Zn^{2+} dissolution in ZnO NP suspensions. Suspensions of ZnO nanoparticles were diluted with MHRW to concentrations equal to the exposure concentrations (See Table 1 for exposure concentrations) and filtered through a Millipore Amicon Ultra-15 filtration device with a molecular weight cutoff of 10 000 Da (Millipore, Billerica, MA). This filter size excludes ZnO particles larger than 2 nm. Therefore, the Zn measured in the filtrate of the samples, "filterable Zn," is the maximum [Zn^{2+}], and soluble Zn is operationally defined as being Zn measured in a solution which has been passed through a 2 nm filter. The Zn unable to pass through the filter, "unfilterable Zn," is considered NPs, although the particles may be present in aggregates larger than 100 nm. Unfiltered suspensions and solutions of $ZnSO_4$ were also analyzed for total Zn content to determine Zn ion recovery, which was over 90%. To determine if additional dissolution would be expected during our exposures, ZnO suspensions were incubated at 25 °C for 24 h to mimic the exposure conditions (without animals). Following incubation, suspensions were filtered and both filtered and unfiltered suspensions were analyzed for total Zn content. All suspensions and solutions were filtered in triplicate and then analyzed. In addition to the filtration experiments, the system ($ZnO_{(solid)}$ in MHRW) was analyzed by a thermodynamic equilibrium model (MINEQL+, Version 4.6).

RNA Isolation and Microarray Hybridization. Following the exposures, *D. magna* were immersed in Tri Reagent, and RNA isolation proceeded according the manufacture's pro-

tocols (Molecular Research Center, Cincinnati, OH). Each exposed RNA was matched with the untreated control RNA harvested on the same date for the microarray hybridizations. Before proceeding to reverse transcription, RNA from both the unexposed and exposed *D. magna* was split into two pools, to provide two dye-swapped technical replicates for each exposure. Because three exposures were performed for each treatment, and RNA from each exposure was hybridized to two different microarrays, there were six hybridizations for each exposure condition. Aminoallyl-labeled dUTP (Applied Biosystems/Ambion, Austin, TX) was incorporated during reverse transcription with M-MuLV reverse transcriptase (New England Biolabs, Ipswich, MA), and flourescence labeling proceeded by incubating the aminoallyl-labeled cDNA with Cy5 or Cy3 fluorescent dyes (GE Healthcare, Piscataway, NJ). Labeled cDNA from the exposed and matched unexposed *D. magna* cDNA was mixed and hybridized to a *D.* magna cDNA microarray containing approximately 7500 random, unsequenced cDNAs. Because additional sequence information was not available at the time of microarray construction to select for specific genes representing functional groups, all available cDNAs were printed. Scanning was performed on an Axon GenePix 4000B microarray scanner (Molecular Devices/MDS Analytical Technologies, Sunnyvale, CA). Reverse transcription of RNA, microarray hybridization methods and additional details related to the construction of the *D. magna* microarray have been described previously (*20*) and are available in the Supporting Information. Information about the experimental design, raw signal intensity values, and other MAIME compliant data are available at the Gene Expression Omnibus (GEO) (located at http://www.ncbi.nlm.nih.gov/geo) with accession number GSE22051.

Gene Expression Analysis. Microarray images were analyzed using GenePix Pro 6.1 (Molecular Devices/MDS Analytical Technologies, Sunnyvale, CA). Downstream data analysis was performed using TIGR TM4 (available at www.tm4.org) (*21*). Background-subtracted signal intensities were normalized by total intensity, lowess normalization, and standard deviation normalization using Microarray Data Analysis System ver. 2.19 (MIDAS). MIDAS was also used to check consistency of dye-flipped pairs and to detect outlier genes using slice analysis (*22*). Normalized signal intensities were analyzed using MultiExperiment Viewer ver. 4.3 (MeV) to detect differentially expressed genes using both a one-class *t* test (*23*) and Statistical Analysis for Microarrays (SAM) using a false discover rate (FDR) <10% (*24*). Genes identified as differentially expressed by both methods were selected as candidate differentially expressed genes and sequenced as described in the Supporting Information. Closest protein homologues were determined by translated BLAST searches to the NCBI database (http://greengene.uml.edu/Batch.html) and *D. pulex* genome v1.0 portal (http://genome.jgi-psf.org/Dappu1/Dappu1.home.html). Gene ontology (GO) was also investigated using Blast2GO (www.blast2go.org) (*25*). Predicted functions were assigned to the cDNAs based on both annotation of the closest protein homologue and assigned GO terms.

Quantitative Reverse Transcription PCR of Candidate Biomarkers. Six candidate biomarkers were selected for validation by quantitative reverse transcription PCR (q-RT-PCR) and are listed in Table S1 (Supporting Information) with primer sequences. Relative gene expression of the candidate biomarkers was assayed using the ABI PRISM 7900HT Sequence Detection System (Applied Biosystems, Foster City, CA) as described previously (*15*). Additional methods are available in the Supporting Information.

Results and Discussion

Characterization, Toxicity, and Dissolution of Nanoparticles. Transmission electron microscopy (TEM) was used to confirm size and elemental composition of the commercially purchased nanomaterials. Representative images from the TEM are shown in Figure S1. An average diameter of 27.2 ± 6.7 nm was determined for the ZnO NPs by measuring over 300 particles. For the SiO_x particles, an average diameter was estimated at 26.4 ± 6.1 nm after measuring approximately 100 particles. The particle diameters are slightly larger than the averages reported by the manufacturer (20 nm for ZnO NPs and 15 nm for the SiO_x NPs) but similar for the two particles. The range of particle diameters as shown in parts C and D of Figure S1 revealed the presence of a few very large particles in each suspension; however, the majority of particles are within a 15 nm range. EDS confirmed that the composition of the particles matched the manufacturer's description (see Figure S2).

We performed toxicity tests to determine relative toxicity of the nanoparticles and obtain appropriate concentrations for our exposure studies. Table 1 reports the toxicity end points for ZnO NPs compared with $ZnSO_4$ revealing that ZnO NPs are about an order of magnitude less toxic than $ZnSO_4$. In contrast, Heinlann et al., who used a similar uncoated ZnO NP from an alternate supplier, found ZnO NPs and $ZnSO_4$ had similar toxicity to *D. magna.* Although the LC_{50} reported for $ZnSO_4$ was similar to our value (1.4 mg/L versus 1.3 mg/L), their LC_{50} for ZnO NPs was much lower compared with our value (2.6 mg/L versus 22.5 mg/L) (*9*). Other studies in *D. magna* have reported toxicity values ranging from 0.5 to 13.4 mg/L (*26, 27*). Difference in the age of the organisms, exposure duration, and variations in the preparation and manufacturer of the NP suspensions may account for these differences.

Several reports have suggested that the toxicity of ZnO NPs arises from dissolution of particles and exposure to the resulting Zn^{2+}, not the ZnO NPs (*8, 9, 27, 28*). In studies with the microalgae *Pseudokirchneriella subcapitata,* Franklin et al. showed, at the IC_{50} for *P. subcapitata* (68 μg/L), total Zn concentration in the ZnO NP suspensions was equal to the dissolved Zn concentration implying that the ZnO NPs were dissolved (*8*). However, with many organisms experiencing toxicity at higher NP concentrations (>1 mg/L), it is unclear whether ZnO NPs are fully dissolved at these concentrations. Additionally, observations of *D. magna* exposed to ZnO NPs at $^1/_{10}$ LC_{50} and LC_{25} illustrate that the particles accumulate on the carapace and appendages of the organisms impeding their ability to swim (see Figure S3). These observations and reports in other organisms including copepods (*11*), zebrafish (*12*), plants, (*10*) and cell lines (*29, 30*) caused us to question the hypothesis that ZnO NP toxicity to *D. magna* was due solely to NP dissolution.

Ultrafiltration was used to determine the concentration of Zn^{2+} in our nanoparticle suspensions. As shown in Figure 1, a portion of zinc in ZnO NPs preparation was present as Zn^{2+} and was able to pass through the filter. This amount, approximately 0.4 mg/L, was similar regardless of the concentration of the NP suspension, and dissolution did not increase over the exposure duration (24 h). Thus, the operationally defined soluble Zn was assumed to be 0.4 mg/L for the exposures. Because the LC_{50} for Zn^{2+} is 1.3 mg/L, and there is a concentration of 0.4 mg/L Zn^{2+} in the ZnO NP suspension, the Zn^{2+} does not account for the total toxicity in our experiments.

Several factors including pH and the presence of other ions in aqueous media govern the solubility of bulk ZnO. When investigating toxicity of ZnO NPs to *D. magna*, Heinlaan et al. used a bacterial biosensor to determine ZnO dissolution in their nanoparticle suspensions. They found that nearly all Zn was bioavailable to the bacteria and suggested it

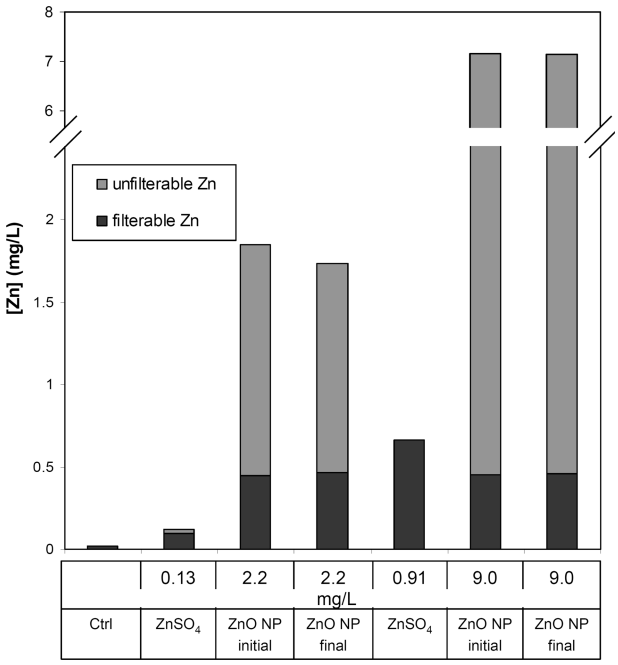

FIGURE 1. Ultrafiltration of ZnO NP suspensions. Suspensions of ZnO NPs and solutions of $ZnSO_4$ were diluted with MHRW to concentrations equal to LC_{25} and $^1/_{10}$ LC_{50} for *D. magna.* Aliquots of these dilutions were filtered through a Millipore Amicon Ultra-15 filtration device as described in the Materials and Methods section. Total zinc content was determined in both the initial suspensions/solutions and the filtrate. The amount of Zn measured in the filtrate is shown in dark gray as "filterable Zn" and represents the operationally defined soluble Zn in this study. The amount of Zn in the initial suspension/solution minus the Zn measured in the filtrate is shown in light gray as "unfilterable Zn" and represents the amount of Zn present as NPs. The height of each bar graph represents the total zinc in the initial suspensions/solutions and is a summation of the filterable and unfilterable Zn. (Because the recovery was not 100% in all initial suspensions, the height of bar graphs is not equal to the nominal concentrations.) ZnO NP suspensions were incubated at 25 °C for 24 h to mimic the exposure duration of the toxicity tests. Zn measured in the suspensions and filtrate prior to incubation is shown as "ZnO NP initial." Zn measured in the suspensions and filtrate following incubation is shown as "ZnO NP final." All suspensions and solutions were filtered and analyzed in triplicate.

represented dissolved Zn^{2+}. However, the pH used in the biosensor assay was lower than our exposures (6.5 compared with 8.1 here) and may explain the differences in ZnO NP dissolution. To better understand the effect of pH on ZnO dissolution, we modeled the equilibrium concentrations of Zn^{2+} in MHRW over a pH gradient using MINEQL+ (Version 4.6). Results from this modeling show that, based on thermodynamic equilibrium, Zn^{2+} concentrations vary within the pH range of our exposures, 7.7−8.2 (see Figure S4) but are within an order of magnititude of the Zn^{2+} concentrations determined through ultrafiltration. In addition, the modeled Zn^{2+} concentrations do not consider the kinetics of dissolution. Thus, within the time frame of the *D. magna* exposures, we conclude that the measured values are the best estimate for actual Zn^{2+} concentrations. Therefore, the *D. magna* are exposed to a mixture of Zn^{2+} and ZnO NPs, with both contributing to the toxicity observed and the resulting gene expression profiles.

Nanoparticle Specific Gene Expression. To explore the differences between the nanoparticles and the corresponding metal ions and develop exposure biomarkers, we used microarrays to investigate gene expression changes after nanoparticle exposure. Two concentrations were chosen for this study: a sublethal (1/10th LC_{50}) concentration and a concentration approaching lethality (LC_{25}, the highest exposure concentration possible to ensure adequate live organisms for downstream gene expression analysis). This allowed comparison of gene expression responses at low and high concentrations. Although we did not explicitly measure the toxicity of $ZnSO_4$ or ZnO NPs at 1/10th LC_{50}, previous work with metal toxicants has shown that chronic toxicity is common at this exposure level (*31*). We also included exposures to SiO_x NPs of a similar size to the ZnO NPs to differentiate between genes responding specifically to the ZnO NPs and genes responding to the presence of a nanosized particle. SiO_x NPs were selected due to their low toxicity compared with ZnO NPs (*19*). Table S2 lists all the genes differentially expressed in the ZnO NP, $ZnSO_4$, and SiO_x exposures organized according the predicted function of the genes. Of the 51 genes responding to the ZnO NP exposures and 40 genes responding to the $ZnSO_4$ exposures, only four overlapped in the gene expression profiles of these treatments. At both concentrations of SiO_x NPs, seven genes were differentially expressed, with only one responding to the ZnO NP exposures. Although not all differentially expressed genes are expected to be directly related to the MOA of these toxicants, because so few genes overlap, the expression profiles suggest that the ZnO NPs cause effects through a mechanism distinct from both Zn ions and SiO_x NPs. These results are consistent with other studies. Griffitt et al. investigated histological and gene expression responses in zebrafish exposed to Cu NPs, Ag NPs, and TiO_2 NPs or concentrations of the metal ions equal to those measured in the NP suspensions. Histology revealed that the metal ion exposures failed to elicit an equivalent degree of toxicity compared with the NPs. In addition, NP and metal ion exposures produced distinct gene expression profiles, providing further evidence that the NPs themselves were causing toxicity to zebrafish (*14*).

Since ZnO NPs produce a unique gene expression pattern, gene expression may provide a method for monitoring and identifying nanomaterials in the environment. Therefore, we identified a subset of differentially expressed genes for biomarker development using quantitative reverse transcription PCR (q-RT-PCR). Genes were selected based on the following: specificity to the NP exposure, variability in gene expression under different conditions, and extent of differential expression. Based on these criteria, the following six genes were selected for confirmation by q-RT-PCR: multicystatin domain containing gene (ES408188), ferritin 3 (AJ292556), a gene similar to gemin7 (GW707335), C1q domain containing gene (GW707341), a putative sodium dependent nucleoside transporter (GW70732), and a gene with no known homologues (GW707356). (The Supporting Information provides a description of the predicted functions of these genes.)

To confirm differential expression of the candidate biomarker genes, four additional exposures were performed for each condition. Because the NP suspensions contained approximately 0.4 mg/L Zn^{2+}, we also performed a $ZnSO_4$ exposure at this concentration to verify that the differential expression was not due the presence of the Zn^{2+}. As shown in Table 2 and Figure S5, the q-RT-PCR and microarray results are in close agreement. The multicystatin, ferritin, and GW707341 were confirmed as differentially expressed. The other three genes, although they had similar expression ratios in the microarray and q-RT-PCR assays, were not shown to be significantly differentially expressed by q-RT-PCR in these four independent exposures. The differential gene expression for multicystatin and ferritin was specific for the NP exposure and not due to the Zn^{2+} present in the suspensions as shown by a lack of differential expression at 0.4 mg/L $ZnSO_4$. GW707341 was differentially expressed in both the ZnO NP

TABLE 2. Gene Expression Ratios of Candidate Biomarker Genes in Microarray and q-RT-PCR Assays Compared with Untreated Controls[a]

predicted function	GenBank acc. no.		ZnO 2.2 mg/L	ZnO 9.0 mg/L	ZnSO4 0.13 mg/L	ZnSO4 0.40 mg/L	ZnSO4 0.91 mg/L
multicystatin	ES408188	uarray	0.202	**0.732**	0.044	NP	0.724
		qPCR	**0.811**	**1.43**	−0.253	0.278	0.322
ferritin	AJ292556	uarray	−0.355	−0.528	−0.151	NP	−0.011
		qPCR	−1.692	−1.906	−0.746	−1.392	−0.812
C1q domain protein	GW707341	uarray	−0.281	−0.863	−0.317	NP	−0.701
		qPCR	−2.514	−2.390	−0.533	−1.271	−0.763
nucleoside transporter	GW707328	uarray	−0.215	−0.329	−0.039	NP	−0.594
		qPCR	−0.107	−0.541	−0.296	−0.463	−0.429
unknown	GW707356	uarray	**0.501**	0.250	0.066	NP	−0.125
		qPCR	0.376	0.297	−0.009	−0.298	−0.048
similar to gemin-7	GW707335	uarray	0.114	**0.590**	0.030	NP	−0.113
		qPCR	0.215	−0.052	0.173	−0.445	−0.452

[a] *D. magna* were exposed to ZnO NP or $ZnSO_4$ at concentrations equal to $^1/_{10}$ LC_{50} and LC_{25} for 24 h. Following the exposures, RNA was isolated and reverse transcribed. q-RT-PCR was carried out on the cDNA using SYBR Green as described in the Materials and Methods section. Log_2 ratios averaged from four replicate q-RT-PCR experiments are compared to the averaged log_2 ratios for the microarray experiments. For microarrays, significance was determined as described in the Materials and Methods section. For q-RT-PCR, significance was determined by *t* test with $p < 0.05$. Genes significantly differentially expressed for a given condition are shown in bold for upregulated genes or underline for downregulated genes. Microarray analysis of gene expression was not performed for 0.40 mg/L $ZnSO_4$ and is represented in the table as "NP." Graphs of the expression levels of each gene including standard deviation are shown in Figure S4 in the Supporting Information.

and $ZnSO_4$ exposures; however, the extent of downregulation was much greater for the NPs. These genes were not differentially expressed by Ag NPs based on preliminary results of a companion study (data not shown), providing further evidence of their specificity for ZnO NPs. However, they must be further evaluated over a range of concentrations and time points and with other common environmental pollutants before they may be used in monitoring programs.

Taken together, the differential gene expression patterns and confirmed expression of the biomarker genes demonstrate that ZnO NPs account for the majority of the toxicity in ZnO NP suspensions to *D. magna*. Following further validation, the three biomarker genes will aid in detecting exposure to NPs and distinguishing between ionic and NP exposures in the environment.

Investigation of ZnO NP Mode of Action. In addition to identifying exposure biomarkers, the microarray approach produces patterns of differential gene expression suggestive of possible MOAs for a toxicant. The expression pattern of ZnO NPs provides additional insight into NP uptake, oxidative stress response, effects to cellular respiration, and reproductive impairment.

Particle Uptake. In order for ZnO NPs to produce toxicity, they must have a mechanism for absorption and cellular uptake. Xia et al. suggest that solid ZnO NPs enter cells through endocytosis and accumulate in lysosomes of macrophages. Smaller particles dissolve in the acidic conditions of the lysosome releasing Zn^{2+} (*29*). After ZnO NP exposure, Kennedy et al. observed electron dense particles in membrane-bound vesicles within human vascular cells also suggesting that the particles are taken up by endocytosis (*30*). In whole organisms, endocytosis and accumulation of fullerenes into lysosomes was observed in the heptapancrease of oysters (*32*). One class of genes upregulated in the present study by ZnO NPs encode proteins involved in the movement of membrane-bound organelles and vesicles including dynactin (GW707365), myosin alkali light chain (GW707407), and restin-like protein (GW707411) (see "cytoskeletal transport proteins" in Table S2). If NPs are taken up by endocytosis as described in the previous studies, the upregulation of cytoskeletal transport genes may be related to movement of NP-containing endosomes to lysosomes.

Oxidative Stress. Cell line studies on ZnO NPs point to oxidative stress leading to lipid peroxidation, membrane leakage, disruption of Ca^{2+} homeostasis, and ultimately apopotosis (*29, 30, 33−35*) as the principle mechanism of toxicity. In vivo studies in isopods and zebrafish support a role for oxidative stress in the toxicity of ZnO NPs (*12, 36*). However, in the present study, several genes which would be anticipated to respond as part of the antioxidant response were not induced, including ferritin 3 (AJ292556) which was instead downregulated (Table 2 and Table S2). It is possible that ZnO nanoparticles act through a distinct mechanism in *D. magna* or elicit oxidative stress after a longer exposure period. However, other studies also found that antioxidant response genes were not induced after ZnO NP exposure. Huang et al. found that only a few of the 84 antioxidant genes on their microarray responded to ZnO NP exposure in human lung epithelial cells (*35*). Zhu et al. observed that although ZnO NP exposure resulted in increased reactive oxygen species (ROS) production, zebrafish embryos failed to initiate an antioxidant response. They inferred that the cell does not recognize ZnO NPs as Zn^{2+} and therefore does not mobilize a response comparable to Zn^{2+} treatments (*12*). However, once inside the cell the NPs are capable of generating ROS and possibly causing increased damage because the antioxidant response is not appropriately initiated.

Cellular Respiration. Genes involved in cellular metabolism were differentially expressed in the ZnO NP exposed *D. magna* (see Table S2). Phosphagens are responsible for buffering inorganic phosphate (P_i) levels and providing additional P_i to ADP in periods of high activity (*37*). The reversible transfer of P_i from arginine phosphate, the primary phosphagen in arthropods, to ADP is catalyzed by arginine kinase (ES408225). This gene was downregulated by the NP exposure, possibly impeding the cell's ability to respond to changing energy needs. Glutamate dehydrogenase (GDH; GW707347) was also downregulated. GDH links glucose and protein metabolism by catalyzing the reversible conversion of α-ketoglutarate to glutamate, and its repression following NP exposure suggests that carbohydrates are being shuttled into the TCA cycle and oxidative phosphorylation. This is supported by the upregulation of two genes involved in the

electron transport chain, cytochrome c oxidase (GW707369) and NADH dehydrogenase (GW713772). The downregulation of both GDH and arginine kinase has been reported in *Gammarus pulex* following PCB exposure suggesting that downregulation of these genes in *D. magna* and resulting alterations in cellular metabolism may be related to a general stress response (*38*).

Reproductive Impairment. The expression level of a number of genes involved in reproduction including vitellogenins (VTGs; AB114859, ES408218, ES408219) and egg shell protein (ES408223) was repressed by both $ZnSO_4$ and ZnO NP exposure (see Table S2). Although these genes were not significantly downregulated in all conditions, their expression ratios are low across the ZnO NP and $ZnSO_4$ treatments. Previous studies have shown that concentrations equal to 0.5 mg/L Zn^{2+} cause a decrease in the fecundity of *D. magna* (*31*). Therefore, the downregulation of these genes may be indicative of reproductive impairment.

In conclusion, our study demonstrated that ZnO NP suspensions contain NPs and Zn^{2+}, and both are likely contributing to the toxicity of ZnO NP suspensions to *D. magna*. The differing gene expression profiles of ZnO NP suspensions and $ZnSO_4$ solutions strongly suggest that the ZnO NPs are causing toxicity through a mechanism distinct from Zn^{2+}. However, transcriptomic studies can only suggest a MOA, and additional mechanistic studies are needed to conclusively demonstrate that ZnO NPs' mechanism of action is separate from $ZnSO_4$. The ZnO NP gene expression profiles revealed effects to cellular respiration and reproduction and provided additional insight into particle uptake and how these NPs exhibit oxidative stress. Three biomarker genes were identified as specific for the ZnO NP exposure providing a promising method for differentiating between exposure to NPs and Zn^{2+} in the environment.

Acknowledgments

The U.S. EPA through its Office of Research and Development funded and managed the research described here. It has been subjected to the Agency's administrative review and approved for publication. We acknowledge the Oak Ridge Institute for Science Education for support. We thank Dr. Jason Unrine of University of Kentucky for his helpful review of this manuscript.

Supporting Information Available

Additional methods details, description of predicted function of biomarker genes, tables and figures; primer sequences for q-RT-PCR (Table S1), complete list of differentially expressed genes (Table S2), TEM images of nanoparticles (Figure S1) with elemental analysis (Figure S2), images of daphnids exposed to ZnO NPs (Figure S3), Zn^{2+} speciation in MHRW as predicted by MINEQL+ (Figure S4), and graphs displaying expression of candidate biomarkers genes (Figure S5). This material is available free of charge via the Internet at http://pubs.acs.org.

Literature Cited

(1) Moore, M. N. Do nanoparticles present ecotoxicological risks for the health of the aquatic environmen? *Environ. Int.* **2006**, *32* (8), 967–76.

(2) Klaine, S. J.; Alvarez, P. J. J.; Batley, G. E.; Fernandes, T. F.; Handy, R. D.; Lyon, D. Y.; Mahendra, S.; McLaughlin, M. J.; Lead, J. R. Nanomaterials in the environment: Behavior, fate, bioavailability, and effects. *Environ. Toxicol. Chem.* **2008**, *27* (9), 1825–1851.

(3) Handy, R. D.; Owen, R.; Valsami-Jones, E. The ecotoxicology of nanoparticles and nanomaterials: Current status, knowledge gaps, challenges, and future needs. *Ecotoxicology* **2008**, *17* (5), 315–325.

(4) Hassellov, M.; Readman, J. W.; Ranville, J. F.; Tiede, K. Nanoparticle analysis and characterization methodologies in environmental risk assessment of engineered nanoparticles. *Ecotoxicology* **2008**, *17* (5), 344–361.

(5) Nohynek, G. J.; Antignac, E.; Re, T.; Toutain, H. Safety assessment of personal care products/cosmetics and their ingredients. *Toxicol. Appl. Pharmacol.* **2010**, *243* (2), 239−259.

(6) Li, Q.; Mahendra, S.; Lyon, D. Y.; Brunet, L.; Liga, M. V.; Li, D.; Alvarez, P. J. Antimicrobial nanomaterials for water disinfection and microbial control: Potential applications and implications. *Water Res.* **2008**, *42* (18), 4591–602.

(7) Hanley, C.; Layne, J.; Punnoose, A.; Reddy, K. M.; Coombs, I.; Coombs, A.; Feris, K.; Wingett, D. Preferential killing of cancer cells and activated human T cells using ZnO nanoparticles. *Nanotechnology.* **2008**, *19* (29), 295103.

(8) Franklin, N. M.; Rogers, N. J.; Apte, S. C.; Batley, G. E.; Gadd, G. E.; Casey, P. S. Comparative toxicity of nanoparticulate ZnO, bulk ZnO, and ZnCl2 to a freshwater microalga (Pseudokirchneriella subcapitata): The importance of particle solubility. *Environ. Sci. Technol.* **2007**, *41* (24), 8484–90.

(9) Heinlaan, M.; Ivask, A.; Blinova, I.; Dubourguier, H. C.; Kahru, A. Toxicity of nanosized and bulk ZnO, CuO and TiO_2 to bacteria *Vibrio fischeri* and crustaceans *Daphnia magna* and *Thamnocephalus platyurus*. *Chemosphere* **2008**, *71* (7), 1308–16.

(10) Lin, D.; Xing, B. Root uptake and phytotoxicity of ZnO nanoparticles. *Environ. Sci. Technol.* **2008**, *42* (15), 5580–5.

(11) Wong, S. W.; Leung, P. T.; Djurisic, A. B.; Leung, K. M., Toxicities of nano zinc oxide to five marine organisms: Influences of aggregate size and ion solubility. *Anal. Bioanal. Chem.* **2010**, *396* (2), 609−18.

(12) Zhu, X.; Wang, J.; Zhang, X.; Chang, Y.; Chen, Y. The impact of ZnO nanoparticle aggregates on the embryonic development of zebrafish (*Danio rerio*). *Nanotechnology* **2009**, *20* (19), 195103.

(13) Poynton, H. C.; Vulpe, C. D. Ecotoxicogenomics: Emerging technologies for emerging contaminants. *J. Am. Water Resource Assoc.* **2009**, *45* (1), 83–96.

(14) Griffitt, R. J.; Hyndman, K.; Denslow, N. D.; Barber, D. S. Comparison of molecular and histological changes in zebrafish gills exposed to metallic nanoparticles. *Toxicol. Sci.* **2009**, *107* (2), 404–15.

(15) Poynton, H. C.; Zuzow, R.; Loguinov, A. V.; Perkins, E. J.; Vulpe, C. D. Gene expression profiling in *Daphnia magna,* Part II: Validation of a copper specific gene expression signature with effluent from two copper mines in California. *Environ. Sci. Technol.* **2008**, *42* (16), 6257–63.

(16) USEPA. *Methods for Measuring the Acute Toxicity of Effluents and Receiving Waters to Freshwater and Marine Organisms*; EPA/812/R/02/012; Office of Water: Washington, DC, 2002.

(17) USEPA. Method 3051: Microwave assisted acid dissolution of sediments, sludges, soils, and oils. In *SW846 Test Methods for Evaluating Solid Waste, Physical/Chemical Methods*; U.S. Government Printing Office: Washington, DC, 1997.

(18) Agency, U. E. P. *Short-Term Methods for Estimating the Chronic Toxicity of Effluents and Receiving Waters to Freshwater Organisms*; EPA-821-R-02−013; U.S. Environmental Protection Agency: Washington, DC, 2002.

(19) Adams, L. K.; Lyon, D. Y.; McIntosh, A.; Alvarez, P. J. Comparative toxicity of nano-scale TiO_2, SiO_2 and ZnO water suspensions. *Water Sci. Technol.* **2006**, *54* (11−12), 327–34.

(20) Garcia-Reyero, N.; Poynton, H. C.; Kennedy, A. J.; Guan, X.; Escalon, B. L.; Chang, B.; Varshavsky, J. R.; Loguinov, A. V.; Vulpe, C. D.; Perkins, E. J. Biomarker discovery and transcriptomic responses in *Daphnia magna* exposed to munitions constituents. *Environ. Sci. Technol.* **2009**, *43* (11), 4188–93.

(21) Saeed, A. I.; Sharov, V.; White, J.; Li, J.; Liang, W.; Bhagabati, N.; Braisted, J.; Klapa, M.; Currier, T.; Thiagarajan, M.; Sturn, A.; Snuffin, M.; Rezantsev, A.; Popov, D.; Ryltsov, A.; Kostukovich, E.; Borisovsky, I.; Liu, Z.; Vinsavich, A.; Trush, V.; Quackenbush, J. TM4: A free, open-source system for microarray data management and analysis. *Biotechniques* **2003**, *34* (2), 374–8.

(22) Quackenbush, J. Microarray data normalization and transformation. *Nat. Genet.* **2002**, *32*, 496–501; Supplement.

(23) Pan, W. A comparative review of statistical methods for discovering differentially expressed genes in replicated microarray experiments. *Bioinformatics* **2002**, *18* (4), 546–54.

(24) Tusher, V. G.; Tibshirani, R.; Chu, G. Significance analysis of microarrays applied to the ionizing radiation response. *Proc. Natl. Acad. Sci. U. S. A.* **2001**, *98* (9), 5116–21.

(25) Conesa, A.; Gotz, S.; Garcia-Gomez, J. M.; Terol, J.; Talon, M.; Robles, M. Blast2GO: A universal tool for annotation, visualization and analysis in functional genomics research. *Bioinformatics* **2005**, *21* (18), 3674–6.

(26) Zhu, X.; Zhu, L.; Chen, Y.; Tian, S. Acute toxicities of six manufactured nanomaterial suspensions to *Daphnia magna*. *J. Nanopart. Res.* **2009**, *11*, 67–75.
(27) Wiench, K.; Wohlleben, W.; Hisgen, V.; Radke, K.; Salinas, E.; Zok, S.; Landsiedel, R. Acute and chronic effects of nano- and non-nano-scale TiO(2) and ZnO particles on mobility and reproduction of the freshwater invertebrate *Daphnia magna*. *Chemosphere* **2009**, *76* (10), 1356–65.
(28) Ma, H.; Bertsch, P. M.; Glenn, T. C.; Kabengi, N. J.; Williams, P. L. Toxicity of manufactured zinc oxide nanoparticles in the nematode *Caenorhabditis elegans*. *Environ. Toxicol. Chem.* **2009**, *28* (6), 1324–30.
(29) Xia, T.; Kovochich, M.; Liong, M.; Madler, L.; Gilbert, B.; Shi, H.; Yeh, J. I.; Zink, J. I.; Nel, A. E. Comparison of the mechanism of toxicity of zinc oxide and cerium oxide nanoparticles based on dissolution and oxidative stress properties. *ACS Nano* **2008**, *2* (10), 2121–34.
(30) Kennedy, I. M.; Wilson, D.; Barakat, A. I. Uptake and inflammatory effects of nanoparticles in a human vascular endothelial cell line. *Res. Rep. Health Eff. Inst.* **2009**, (136), 3–32.
(31) Poynton, H. C.; Varshavsky, J. R.; Chan, S.; Loguinov, A. V.; Perkins, E. J.; Vulpe, C. D. Gene expression profiling in *Daphnia magna,* Part I: concentration dependent gene expression profiles provide support for the no observed transcriptional effect level in Daphnia magna. *Environ. Sci. Technol.* **2008**, *42* (16), 6250–6.
(32) Ringwood, A. H.; Levi-Polyachenko, N.; Carroll, D. L. Fullerene exposures with oysters: Embryonic, adult, and cellular responses. *Environ. Sci. Technol.* **2009**, *43* (18), 7136–41.
(33) Jeng, H. A.; Swanson, J. Toxicity of metal oxide nanoparticles in mammalian cells. *J. Environ. Sci. Health, Part A: Toxic/Hazard. Subst. Environ. Eng.* **2006**, *41* (12), 2699–2711.
(34) Yang, H.; Liu, C.; Yang, D.; Zhang, H.; Xi, Z. Comparative study of cytotoxicity, oxidative stress and genotoxicity induced by four typical nanomaterials: The role of particle size, shape and composition. *J. Appl. Toxicol.* **2009**, *29* (1), 69–78.
(35) Huang, C. C.; Aronstam, R. S.; Chen, D. R.; Huang, Y. W. Oxidative stress, calcium homeostasis, and altered gene expression in human lung epithelial cells exposed to ZnO nanoparticles. *Toxicol. In Vitro* **2010**, *24*, 45–55.
(36) Valant, J.; Drobne, D.; Sepcic, K.; Jemec, A.; Kogej, K.; Kostanjsek, R. Hazardous potential of manufactured nanoparticles identified by in vivo assay. *J. Hazard. Mater.* **2009**, *171* (1−3), 160–5.
(37) Ellington, W. R. Evolution and physiological roles of phosphagen systems. *Annu. Rev. Physiol.* **2001**, *63*, 289–325.
(38) Leroy, D.; Haubruge, E.; De Pauw, E.; Thome, J. P.; Francis, F. Development of ecotoxicoproteomics on the freshwater amphipod *Gammarus pulex*: Identification of PCB biomarkers in glycolysis and glutamate pathways. *Ecotoxicol. Environ. Saf.* **2010**, *73* (3), 343–52.

ES102501Z